



ELSEVIER

Contents lists available at ScienceDirect

Nuclear Instruments and Methods in Physics Research A

journal homepage: www.elsevier.com/locate/nima

Optical, luminescence and thermal properties of radiopure ZnMoO₄ crystals used in scintillating bolometers for double beta decay search

D.M. Chernyak^{a,b}, F.A. Danevich^a, V.Ya. Degoda^c, I.M. Dmitruk^c, F. Ferri^d, E.N. Galashov^e, A. Giuliani^{b,d,g,*}, I.M. Ivanov^e, V.V. Kobychiev^a, M. Mancuso^{b,d}, S. Marnieros^{b,d}, V.M. Mokina^a, C. Nones^f, E. Olivieri^b, G. Pessina^g, C. Rusconi^{d,g}, V.N. Shlegel^e, O.P. Stanovyi^c, M. Tenconi^b, V.I. Tretiyak^a, I.A. Tupitsyna^h

^a Institute for Nuclear Research, MSP 03680 Kyiv, Ukraine

^b Centre de Sciences Nucléaires et de Sciences de la Matière, 91405 Orsay, France

^c Kyiv National Taras Shevchenko University, MSP 03680 Kyiv, Ukraine

^d Dipartimento di Scienza e Alta Tecnologia dell'Università dell'Insubria, Como I-22100, Italy

^e Nikolaev Institute of Inorganic Chemistry, 630090 Novosibirsk, Russia

^f Service de Physique des Particules, CEA-Saclay, F-91191 Gif sur Yvette, France

^g Sezione INFN di Milano-Bicocca, I-20126 Italy

^h Institute of Scintillation Materials, 61001 Kharkiv, Ukraine

ARTICLE INFO

Article history:

Received 20 March 2013

Received in revised form

25 July 2013

Accepted 31 July 2013

Available online 29 August 2013

Keywords:

Double beta decay

¹⁰⁰Mo

Cryogenic scintillating bolometer

ZnMoO₄ crystal

ABSTRACT

Zinc molybdate (ZnMoO₄) crystals are an excellent candidate material to fabricate scintillating bolometers for the study of neutrinoless double beta decay of ¹⁰⁰Mo, provided that the crystal quality meets strict optical, thermal and radiopurity requirements. This paper addresses the characterization of improved crystalline samples grown by the low-thermal-gradient Czochralski technique. Transmittance measurements confirm significant improvement of the material with respect to previously developed samples. Luminescence properties (emission spectra, dependence of intensity on temperature, thermally stimulated luminescence and phosphorescence) have been studied under X-ray excitation from liquid-helium to room temperature. The index of refraction was measured in the wavelength interval 406–655 nm. Samples of ZnMoO₄ crystals with masses of 5.07 g and 23.8 g were operated as scintillating bolometers at temperatures below 30 mK, with simultaneous detection of scintillation and heat signals, confirming an excellent alpha/beta rejection power. Background measurements allowed encouraging radiopurity level estimations. The light collection from ZnMoO₄ scintillators was Monte Carlo simulated, analysing different crystal size, shape and surface properties and different photodetector sizes.

© 2013 Elsevier B.V. All rights reserved.

1. Introduction

Neutrinoless double beta ($0\nu 2\beta$) decay is a key process in contemporary particle physics thanks to its unique ability to test the Majorana nature of neutrino and lepton number conservation, the absolute scale and the hierarchy of neutrino mass, the existence of right-handed currents in the weak interaction and hypothetical Nambu–Goldstone bosons (the so-called Majorons) [1–5].

The quasi-degenerate neutrino mass pattern is almost discarded by the most precise experiments. To start testing the inverted neutrino mass hierarchy scenario, $0\nu 2\beta$ experiments should be sensitive to the effective Majorana neutrino mass

$\langle m_\nu \rangle \sim 0.05$ eV, where the theoretically predicted half-lives are within 10^{26} – 10^{27} years even for the most promising candidate nuclei (see e.g. the review [4]). To discover (exclude) the inverted hierarchy pattern one should advance the experimental sensitivity to the level of $\langle m_\nu \rangle \sim 0.01$ – 0.02 eV, which corresponds to $T_{1/2} \sim 10^{27}$ – 10^{28} years. Radioactivity with a half-life of 10^{27} years means a few decays in 100 kg of isotope over 5 years (e.g., 1.4, 2.1 and 4.3 decays for ¹⁵⁰Nd, ¹⁰⁰Mo and ⁴⁸Ca, respectively). Observation of such a low activity requires detectors with high detection efficiency and energy resolution, and very low (ideally zero) background.

In order to provide high detection efficiency and spectrometric characteristics, a choice of nuclei is required. Relevant nuclei are determined by the scale of experiments (hundred kilograms of isotope of interest), extreme requirements on background and possibility of calorimetric experiments (source=detector). Considering some of the most appealing nuclei from the point of view

* Corresponding author at: Centre de Sciences Nucléaires et de Sciences de la Matière, 91405 Orsay, France. Tel.: +33 169155526.

E-mail address: Andrea.Giuliani@csnsm.in2p3.fr (A. Giuliani).

of nuclear theory, mass production is available for ^{76}Ge , ^{82}Se , ^{100}Mo , ^{116}Cd , ^{130}Te and ^{136}Xe [6], while a suppression of the background to a level compatible with extremely low activity looks more realistic for the isotopes with the energy of double beta decay above that of the edge of natural radioactivity at 2615 keV (γ quanta from decay of ^{208}Tl , in the chain of ^{232}Th). Only ^{82}Se , ^{100}Mo and ^{116}Cd pass this filter and, fortunately, there is a proper instrument to investigate these isotopes: scintillating low temperature detectors [7–13] providing high detection efficiency (70–90%, depending on crystal scintillator composition and size) and energy resolution (a few keV). In addition, this technique is able to suppress background caused by internal and surface radioactive contamination of crystal scintillators to a very low level thanks to its excellent particle discrimination.

The isotope ^{100}Mo is one of the most promising candidates in the search for $0\nu2\beta$ decay thanks to the high energy of the decay ($Q_{2\beta} = 3034.40(17)$ keV [14]), comparatively high natural isotopic abundance ($\delta = 9.824(50)\%$ [15]) and the favorable theoretical predictions [16–24]. The $2\nu2\beta$ decay of ^{100}Mo was measured with the greatest precision by the NEMO 3 collaboration [25] which gave the value of $T_{1/2} = (7.11 \pm 0.54) \times 10^{18}$ years. The $0\nu2\beta$ decay of ^{100}Mo has not been observed to date: the best half-life limit was obtained in the NEMO 3 experiment as $T_{1/2} \geq 10^{24}$ years at 90% C.L. [26].

There are several possibilities for low temperature crystal scintillators containing molybdenum: Li_2MoO_4 [27,28], $\text{Li}_2\text{Zn}_2(\text{MoO}_3)_4$ [29], CaMoO_4 [8,30–33], SrMoO_4 [8], CdMoO_4 [8,34], PbMoO_4 [8,35–37]. Zinc molybdate (ZnMoO_4) is one of the most promising materials for the search for $0\nu2\beta$ decay of ^{100}Mo thanks to the absence of long-lived radioactive isotopes of constituting elements and comparatively high percentage of molybdenum (43% in weight). The main properties of ZnMoO_4 crystal scintillators are presented in Table 1.

A small ZnMoO_4 single crystal was grown and its crystal structure was studied 50 years ago [40,44]. This compound in the form of polycrystals was identified in Ref. [42] as a suitable scintillation material for cryogenic detectors, including the search for neutrinoless double beta decay of ^{100}Mo . Comparatively large single ZnMoO_4 crystals grown for the first time by the Czochralski and Kyropoulos methods were reported in Ref. [38]. Single crystal samples 20–30 mm in diameter and 30–40 mm in height were then produced using the Czochralski technique [41]. Properties of the ZnMoO_4 crystal as low temperature scintillating bolometers were tested for the first time in Ref. [45]. However the crystals produced in Ref. [38,41] were of an intense yellow colour. This feature led to absorption of scintillation light and, as a result, to lower light output and nonuniformity of light collection in the light channel of the scintillating bolometers. Furthermore, the polycrystalline structure of the samples produced earlier (see Section 3.1.2) could deteriorate the bolometric properties of the material.

The purpose of our work was the study of the features of ZnMoO_4 crystals with improved optical quality as cryogenic scintillating bolometers to search for double beta decay of ^{100}Mo . These improved crystals were already used in well-performing cryogenic detectors [46–48], but no systematic investigation of their properties was performed. The definition of this crucial aspect of the material under discussion is essential for a future large-scale double beta decay experiment, which envisages the routine production on a semi-industrial basis of ZnMoO_4 crystals from ^{100}Mo -enriched raw materials with related well-defined quality-control criteria: low level of radioactive contamination by ^{228}Th and ^{226}Ra (less than 0.01 mBq/kg), optimum bolometric properties, high optical quality (absorption coefficient no less than 30 cm^{-1} at the emission maximum $\approx 600 \text{ nm}$), efficient luminescence at low temperature (≥ 1.5 photons/keV at liquid helium temperature) and large mass (0.2–0.5 kg) [47,48].

We have carried out measurements of light transmission to check the optical properties of the improved material. Index of refraction was measured for wavelengths 406, 532 and 655 nm taking into account the anisotropy of the crystal. The luminescence properties were studied under X-ray irradiation from room to liquid helium temperature. Two samples obtained from the improved ZnMoO_4 crystal were tested as cryogenic scintillating bolometers. Radioactive contamination of one ZnMoO_4 crystal sample was estimated using the cryogenic measurements, in which the light and phonon signals detected simultaneously allow clear discrimination between α and $\beta(\gamma)$ particles. The light collection from ZnMoO_4 crystal scintillators of different size, shape and surface conditions by photodetectors of different sizes was Monte Carlo calculated with the GEANT4 simulation package.

2. Production of advanced ZnMoO_4 crystals

ZnMoO_4 crystal of advanced quality was developed in the Nikolaev Institute of Inorganic Chemistry (Novosibirsk, Russia).

Transparency of the crystals depends substantially on the contamination of the initial charge for crystal growth by transition metals, such as V, Cr, Fe, Co. Specifically contamination by Fe may jeopardize the scintillation yield (see Subsection 3.2.1). Therefore a deep purification of raw materials from this kind of impurity is necessary. High-purity molybdenum oxide (MoO_3) to synthesize ZnMoO_4 compound was obtained from molybdenum oxide dissolved in ammonia. Purification of solutions from impurities was carried out by coprecipitation on $\text{Zn}(\text{OH})_2$. Zinc oxide was dissolved in a solution of ammonium molybdate at a pH of 6–7. Adding of ammonium to the solution leads to an increase of pH up to 8–9 and the formation of insoluble compounds of Fe and Zn. The resulting precipitate $\text{Zn}(\text{OH})_2$ absorbs different impurities on its surface. After separation of the precipitates, some volume of

Table 1
Properties of ZnMoO_4 crystal scintillators (SR denotes Synchrotron Radiation).

Property	Value	Measurements conditions	Reference
Density (g/cm^3)	4.3		[38]
Melting point ($^\circ\text{C}$)	1003 ± 5		[38]
Structural type	Triclinic, $P1$		[38,39]
Cleavage plane	Weak (001)		[38]
Hardness on the Mohs scale	3.5		This work
Index of refraction	1.90–1.92 1.89–1.96	For Na light (589 nm) At 532 nm	[40] This work
Wavelength of emission maximum (nm)	605 585 625	SR 6.5 eV, 10 K X-ray excitation, 8 K X-ray excitation, 8 K	[38] [41] This work
Scintillation decay time (μs)	$\approx 1.3, 16, 150$ 3.9	SR 6.5 eV, 80 K SR 5.5 eV, 300 K	[42] [43]

$(\text{NH}_4)_2\text{C}_2\text{O}_4$ was added to the solution to bind ions of Fe and other impurities. The purified solution was evaporated with the release of ammonium molybdate crystals. Molybdenum oxide was obtained by annealing. The content of Na, Ca, Fe, Pb and Zn in the MoO_3 was at the level of < 1 ppm. Contamination of other elements did not exceed the level of 0.1–0.001 ppm. Commercial zinc oxide with an impurity content at the level of $< (0.1\text{--}0.01)$ ppm was used to obtain the ZnMoO_4 compound for crystal growth.

Three ZnMoO_4 crystal boules of improved optical quality (see Fig. 1) were grown in similar conditions and from the same input powder by the low-thermal-gradient Czochralski technique [49–51] in a platinum crucible of size $\varnothing 40 \times 100$ mm. The crystals were grown at a speed of 0.6–0.8 mm/h. The specimens analysed in this work (and compared with previous samples) come from two of these three boules (hence referred to as #1, #2 and #3). In particular, three samples were obtained from boule #1, characterized by a diameter of about 25 mm and a height of about 60 mm. Boule #3 was used to obtain a cylindrical crystal whose performance as scintillating bolometer is described in Ref. [48].

A summary of the features of the samples studied here is provided in Table 2. Crystals No. 3, No. 5 and No. 6 were cut from boule #1, while crystal No. 7 was cut from boule #2 (see Fig. 1).

3. Measurements, results and discussion

3.1. Optical and luminescence properties

3.1.1. Light transmission

The transmittance of three 5 mm thick ZnMoO_4 samples (developed in Ref. [38,41] and in the framework of the present study and referred to as No. 1, 2 and 3 in Table 2) was measured using a commercial fiber optic spectrophotometer (Ocean Optics HR2000CG-UV-NIR) and a deuterium/tungsten-halogen lamp



Fig. 1. Crystal boules #1 (left) and #2 (right) from which some improved samples studied in this work were obtained. The polished cylinder in the center, used to fabricate a scintillating bolometer described in Ref. [48], was obtained from a similar boule #3. The scale is in centimeters.

(Ocean Optics DH 2000). Two multimode optical fibers (200 μm core), coupled with two quartz lenses that act as collimators, were used for shining and collecting the light transmitted by the sample. The use of an optical fiber collimator (which acts as a spatial filter) for the light detection ensures that stray light scattered in the forward direction by crystal surfaces and other impurities does not re-enter the collection optics and, therefore, does not affect the measurement of the transmitted power.

The transmission curves are shown in Fig. 2. The results confirm a significant improvement of the optical quality of the crystal grown from additionally purified raw materials by the low-thermal-gradient Czochralski technique. It should be stressed that samples No. 1 and 2 have shown a substantial difference of transmission when the position of the light beam was scanned over the crystals surface. As well as this, the sample No. 3 has much better homogeneity. The absorption band at $\approx 440\text{--}460$ nm observed in previously produced crystals [38] was explained as being mainly due to Fe impurity [43]. One could assume that the similar behaviour of transmission of the sample [41] is also due to iron contamination of the crystal. Therefore deep purification of raw materials, especially from iron traces, is an important step to obtain clear ZnMoO_4 crystals.

3.1.2. Index of refraction

The refractive index of two ZnMoO_4 samples (No. 4 and 5 in Table 2), one produced earlier in Ref. [41] (No. 4) and the second one of the improved quality developed in the framework of the present study (No. 5), was measured with the help of a GS-5 goniometer. The samples were shaped as triangular prisms. The sample No. 4 has shown a substantial multiple refraction of light. We suppose that it was due to some imperfection of the crystal, probably misoriented block structure. X-ray crystallography

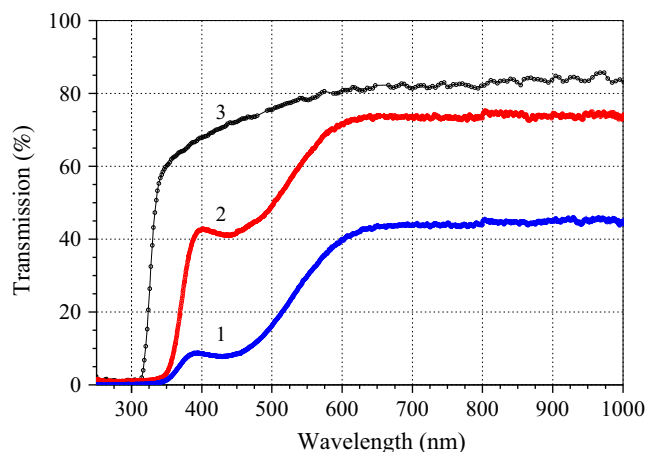


Fig. 2. Optical transmission curve of the improved ZnMoO_4 crystal of thickness 5 mm developed in the present work (3). Data for ZnMoO_4 samples produced in Ref. [38] (1) and in Ref. [41] (2) are given for comparison.

Table 2
Samples used to perform the measurements described in the text. IGP stands for Institute of General Physics (Moscow, Russia), ISMA for Institute for Scintillation Materials (Kharkiv, Ukraine) and NIIC for Nikolaev Institute of Inorganic Chemistry (Novosibirsk, Russia).

No.	Size (mm), mass (g)	Producer	Type of measurement	Reference
1	15 × 15 × 5	IGP	Transmission	[38]
2	15 × 15 × 5	ISMA	Transmission	[41]
3	15 × 15 × 5, 5.07	NIIC	Transmission and scintillating bolometer	This work boule #1
4	Triangular prism 15 × 15 × 5	ISMA	Index of refraction	[41]
5	Triangular prism 15 × 15 × 5	NIIC	Index of refraction	This work boule #1
6	10 × 10 × 2	NIIC	Luminescence	This work boule #1
7	Cylinder $\varnothing 16 \times 28$, 23.8	NIIC	Scintillating bolometer	This work boule #2

measurements are consistent with the hypothesis of a substantial polycrystalline structure of the sample No. 4. As well as this, the measurements confirmed a much better quality of the improved ZnMoO_4 crystal.

Finally the measurements of the improved sample No. 5 were used to derive the refractive index values. It was found that the two refractive indices (for two normal waves with different polarizations) vary over a range of 0.02–0.03 for different directions (see Table 3). The variation indicates that the crystal is biaxial, which is in agreement with triclinic structure of ZnMoO_4 . Indices are presented for three wavelengths in the red, green, and blue parts of visible spectrum. The data do not contradict earlier results [40] where index of refraction 1.90–1.92 was measured with Na light. Some discrepancies can be attributed to the differences in the wavelength and to a wide variation of directions in the present study since the index of refraction depends on: (i) wavelength (because of dispersion), (ii) direction in the crystal (because of anisotropy), (iii) polarization (because of birefringence). We have performed measurements in a wider range of wavelengths and probably in a wider range of directions than that in work [40]. Thus it is not surprising that we obtained a broader range of refractive indices variation.

We have also estimated the hardness of ZnMoO_4 crystals on Mohs scale as 3.5 by a simple scratching test using calcite (hardness on Mohs scale is 3) and fluorite (4).

3.1.3. Luminescence under X-ray excitation

The luminescence of ZnMoO_4 crystal was investigated in the temperature interval 8–290 K under X-ray excitation. A sample of ZnMoO_4 crystal ($10 \times 10 \times 2$ mm, No. 6 in Table 2) was irradiated by X-rays from a BHV7 tube with a rhenium anode (20 kV, 20 mA). Light from the crystal was detected in the visible region by a FEU-106 photomultiplier (sensitive in the wide wavelength region of 300–800 nm) and in the near infrared region by FEU-83 photomultiplier with enhanced sensitivity up to $\approx 1 \mu\text{m}$. Spectral measurements were carried out using a high-aperture MDP-2 monochromator.

Emission spectra measured at 8, 118 and 290 K are shown in Fig. 3. A broad band in the visible region with a maximum at 610 nm was observed at room temperature. At 8 K luminescence exhibits an emission band with a maximum at 625 nm in reasonable agreement with the results of previous studies [38,41,42,52].

The dependence of the integral luminescence intensity, and of the luminescence intensity near the maximum of the emission spectrum as a function of the temperature are presented in Fig. 4. The luminescence is strongly quenched at room temperature. The light output grows with decreasing temperature, reaches a maximum around 110–140 K and then drops with further cooling. This result is again in agreement with the data of previous investigations [42,43].

The sample shows intense thermostimulated luminescence (TSL) at ≈ 75 K (see Fig. 5), which indicates the presence of defects and impurities in the crystal. Phosphorescence observed after irradiation of the sample at the temperature of 8 K (see inset in Fig. 5) also confirms the presence of shallow traps due to

Table 3

Refractive indices n_1 and n_2 of a ZnMoO_4 crystal for two light polarizations (see text for details). The error of the values is ± 0.01 .

Wavelength (nm)	Refractive indexes	
	n_1	n_2
406	1.94–1.97	1.98–2.01
532	1.89–1.91	1.94–1.96
655	1.87–1.90	1.91–1.93

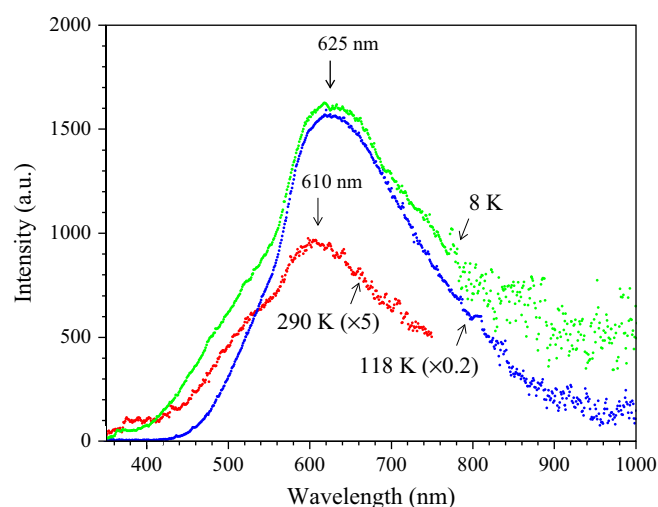


Fig. 3. Emission spectra of ZnMoO_4 crystal under X-ray excitation at the temperatures 290, 118 and 8 K. (For interpretation of the references to color in this figure caption, the reader is referred to the web version of this paper.)

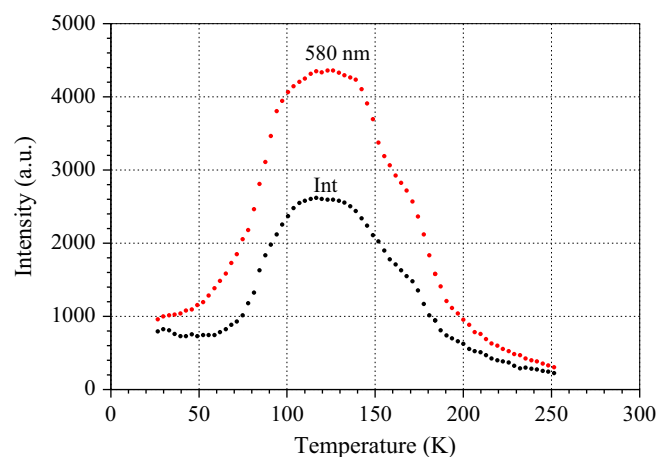


Fig. 4. Dependence of ZnMoO_4 luminescence intensity under X-ray excitation on temperature in wide interval of emission spectrum (Int), and near the maximum of intensity (580 nm).

imperfections in the crystal.¹ Therefore there is still considerable potential to improve the quality of the material.

3.2. Low temperature measurements

3.2.1. Cryogenic and detector setups

The operation of the scintillating bolometers at low temperatures was performed in the cryogenic laboratories of the University of Insubria (Como) and of CSNSM (Orsay). The set-up in Como, in which a scintillating bolometer based on a 5.07 g ZnMoO_4 crystal was installed, consists of a low-power dilution refrigerator, capable of reaching a temperature of 13 mK in the absence of thermal loads. A small experimental space, corresponding to a cylinder about 20 cm high and 4 cm diameter, is available in this cryostat.

The energy absorber of the aforementioned 5.07 g detector (see Fig. 6(a)) was a rectangular single ZnMoO_4 crystal, with size $15 \times 15 \times 5$ mm (sample No. 3 in Table 2). It was contained in a cylindrical copper holder, acting as a heat sink for the detector. The

¹ It should be mentioned that we have observed two decay components in the phosphorescence curves, with decay times of ≈ 2 s and ≈ 360 s.

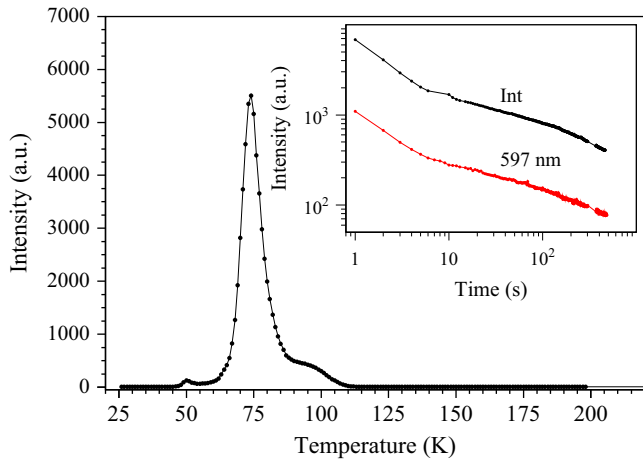


Fig. 5. Thermoluminescence of ZnMoO₄ crystal after X ray excitation at liquid helium temperature. (Inset) Phosphorescence after X ray irradiation at 8 K in wide interval of emission spectrum (Int) and at 597 nm.

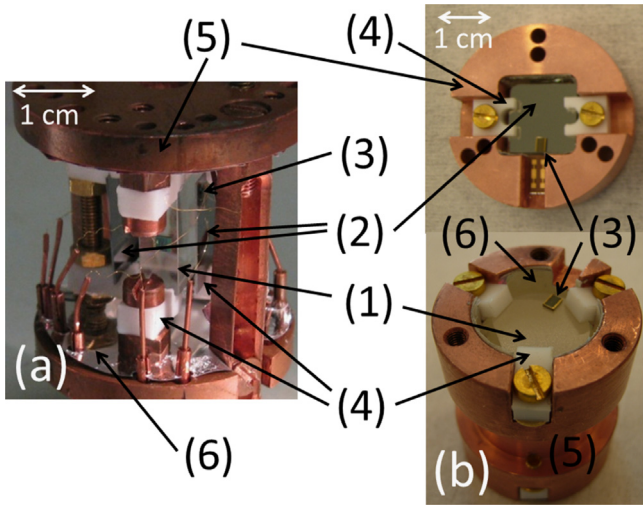


Fig. 6. Photograph of the detectors setup: (a) the 5.07 g detector assembly; (b) the 23.8 g detector assembly with one dismantled light detector to highlight the modular structure. For both setups: (1) ZnMoO₄ crystal; (2) Ge slabs (photodetectors); (3) NTD thermistors; (4) PTFE supporting elements; (5) copper support of the detector; (6) light reflector.

mechanical coupling to the holder was supplied by four PTFE elements. On the two opposite 15 × 15 mm sides, the ZnMoO₄ crystal was faced by two light-detecting square ultrapure Ge crystalline slabs of 15 mm side and 0.5 mm thickness. The light detectors were kept in position by two PTFE pieces, clamping the slabs on two opposite edges.

Heat signals from the ZnMoO₄ crystal and from the Ge slabs were measured with neutron transmutation doped (NTD) germanium thermistors thermally glued to the energy absorbers, chosen so as to have resistances of the order of a few MΩ and a logarithmic sensitivity $-d \log R/d \log T \sim 6$ in the 20–25 mK range. The thermistor mass is of the order of 10 mg.

After operation in Como, the 5.07 g scintillating bolometer was moved to Orsay and tested there. The cryogenic set-up in Orsay consisted of a medium cooling power dilution refrigerator with a large experimental space of a few liters, and characterized by a base temperature of about 15 mK.

In addition to the 5.07 g detector, a larger device was tested in the Orsay apparatus, based on a 23.8 g ZnMoO₄ crystal (sample No. 7 in Table 2). The energy absorber of this scintillating bolometer had an almost cylindrical shape, with a height of 28 mm and a

diameter of 16 mm. Similarly to the smaller detector, the crystal was kept firmly in position by six PTFE elements clamping it at the two bases. Two light detectors, consisting of square hyperpure Ge crystalline slabs with the same area as those used for the 5.07 g bolometer (but with a smaller thickness of 0.3 mm), were facing the ZnMoO₄ crystal at the flat sides. This time each Ge slab had an independent holder, in a configuration similar to that described in Ref. [53] (see Fig. 6(b)). This has allowed a systematic investigation of the light detector properties as well as their separate and individual optimization [54]. The NTD Ge thermistors used for the 23.8 g scintillating bolometer had features similar to those described above for the small detector, but with twice the volume.

3.2.2. Response to γ quanta, α particles and light output

The detectors were put in operation at various base temperatures between 20 and 30 mK in the two aforementioned dilution refrigerators. The best performances were obtained with typical NTD thermistor resistances of the order of 1 MΩ, with bias currents in the range 2–5 nA. The typical temporal structure of the pulses is characterised by risetimes in the 1 ms range and decay times in the 10 ms range. The signals from the NTD thermistors were amplified by low noise voltage amplifiers, with a cold front-end stage in the Orsay set-up only. The data acquisition system enabled registration of the full waveforms of the signals, followed by off-line application of optimum filtering in order to maximize the detector energy resolution.

Plots reporting the light-to-heat signal amplitude ratio versus the heat signal amplitude for each event show an excellent separation between β/γ events and α events for both detectors, as can be appreciated in Fig. 7. The calibration of the light detector was performed using the 5.89 keV and 6.49 keV lines of a ⁵⁵Fe source, while the energy scale of the heat channel was established using gamma sources and background peaks induced by environmental radioactivity. The lines defining the regions containing 99.9% of the events for α and β interactions respectively were computed by considering the uncertainty, as a function of the heat signal amplitude, of the light-to-heat signal amplitude ratio, derived from the intrinsic pulse-amplitude resolution of the heat and light signals (reported in Table 4). The plots show that, with an acceptance of β events practically equal to 1, the α rejection factor is better than 10^{-3} at the energy ≈ 3 MeV. This discrimination is equally achievable for much larger detectors [48,55] and was also demonstrated for the 23.8 g detector described here, but these data are still preliminary and will be reported in a dedicated paper.

The performances of the two detectors are summarized in Table 4. We report the sensitivity of the heat channel S_h , the sensitivities of the two light channels S_{l1} and S_{l2} , the intrinsic energy resolution (in terms of $2.35 \times$ the 1σ baseline fluctuation) of the heat channel E_R , the threshold of the two light channels Th_{l1} and Th_{l2} (reported as $5 \times$ the 1σ baseline fluctuation), the relative light yield LY for β -like particles – obtained by taking into account both light detector responses but neglecting light collection efficiency and reflection losses – and the light (heat) quenching factor Q_l (Q_h) of α particle signals with respect to β particle signals for the same deposited energy (~ 5.4 MeV). The data on light yields and quenching factors could be affected (especially for the 23.8 g detector) by valuable cross-talk between the heat and light channel (corrected off-line). We have estimated the systematic errors for LY, Q_l and Q_h to be at the level of 10%. The differences in the light-yields are not surprising, taking into account the different geometries of the two set-ups. It is more difficult to explain the discrepancy between the heat quenching factors for α particles. However, one should keep in mind that there is still no model able to explain the extent of the excess of the heat signals from α particles. The difficult reproducibility of the light detectors,

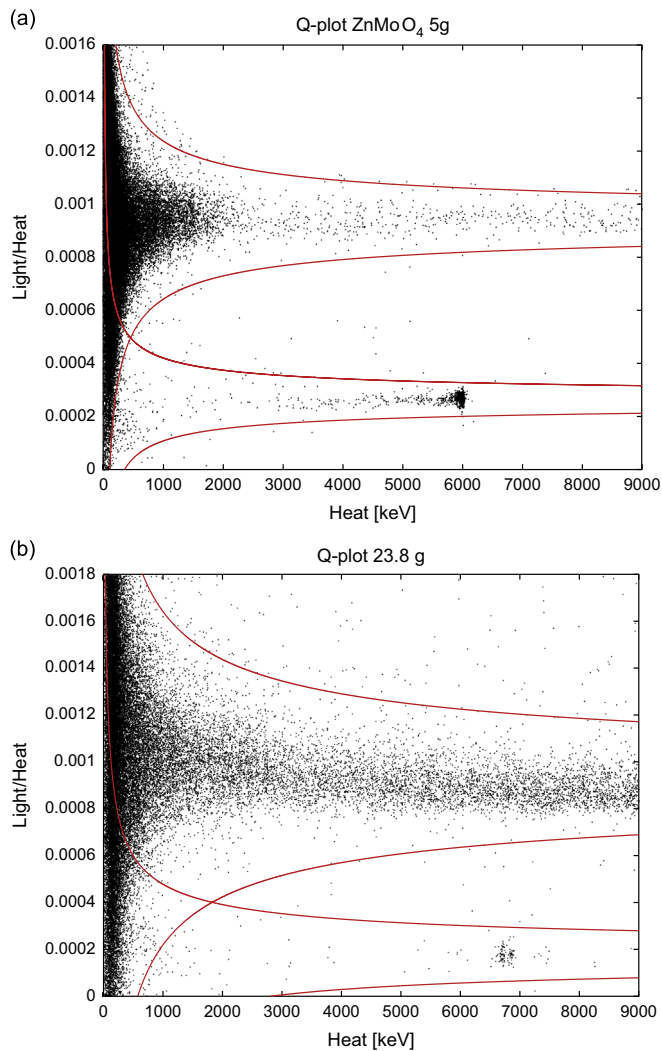


Fig. 7. Plots reporting the light-to-heat signal amplitude ratio as a function of the heat signal amplitude for the 5.07 g (a) and the 23.8 g (b) ZnMoO_4 scintillating bolometers. The two bands related to β/γ events (which also include cosmic muon interactions) and α events are well separated. The α band is populated mainly by a ^{241}Am source (~ 5.4 MeV) for the 5.07 g detector and by a contamination of ^{210}Po (both external and superficial – lower energy line at ~ 5.3 MeV – and internal to the crystal itself – higher energy line at ~ 5.4 MeV) for the 23.8 g detector. The heat energy scale is determined with a γ calibration. The α particle energy is misplaced with respect to this calibration because of a substantial difference in the thermal response between α and β events.

Table 4
Performances of the 5.07 g and 23.8 g ZnMoO_4 detectors. See text for a description of the reported parameters.

Parameter	5.07 g	23.8 g
S_h ($\mu\text{V}/\text{MeV}$)	200	77
S_{h1} ($\mu\text{V}/\text{MeV}$)	2.0	0.21
S_{h2} ($\mu\text{V}/\text{MeV}$)	1.0	0.39
E_R (keV)	0.82	1.5
Th_{11} (eV)	175	974
Th_{12} (eV)	628	314
LY (keV/MeV)	2.1	1.8
Q_l	0.17	0.19
Q_h	1.1	1.3

both in terms of signal amplitude and noise level, is well documented elsewhere [54] and is confirmed by the measurements reported here. However, all the four light detectors used in

this work exhibit performances able to discriminate β and α events.

3.2.3. Radioactive contamination of ZnMoO_4 crystals

In the α band, the background spectrum is characterised by an internal contamination of ^{210}Po at 5410 keV both for the 5.07 g and 23.8 g detectors, while no other α peaks are appreciable over the acquired data samples. The radioactive contamination of the ZnMoO_4 crystal sample was estimated using the data of low-temperature exposure and discrimination between α and $\gamma(\beta)$ events.

A summary of radioactive contamination of the ZnMoO_4 crystals (or limits on their activities) is given in Table 5 where the radioactive contamination of ZnMoO_4 crystals measured in Ref. [45,55] and zinc tungstate (ZnWO_4) crystal scintillator studied in Ref. [56] are given for comparison. The crystal studied in Ref. [55] has a large mass (≈ 330 g) and the test was performed underground at the Gran Sasso National Laboratories of INFN (Italy). This explains the higher sensitivity achieved with this device. This large crystal comes from none of the three boules mentioned in this work, but it was subsequently grown following essentially the same purification and growth procedures. Our data in Table 5 refer to an aboveground 64 h long measurement with the 23.8 g detector (sample No. 7 in Table 2), which provided more stringent limits than those obtained with the 5.07 g detector (sample No. 3 in Table 2) [46]. One can see that the additional purification of molybdenum, used for the synthesis of ZnMoO_4 powder for the improved crystals growth, allowed dramatic reduction of the radioactive impurity content as well. These results are in agreement with those reported in Ref. [48].

The efforts made for the molybdenum purification have improved the radiopurity of ZnMoO_4 crystals to the level of those based on ZnWO_4 , which were initially considerably less contaminated. In particular, one of the ZnWO_4 crystals studied in Ref. [56] was produced from the same initial zinc oxide as used for ZnMoO_4 growth. Comparing these data, it is clear that the purification of molybdenum is a crucial step in order to achieve low radioactive contamination of ZnMoO_4 crystals. This point has to be kept firmly in mind in view of future crystal growths starting from molybdenum enriched in ^{100}Mo .

4. Monte Carlo simulation of the light collection from ZnMoO_4 crystal scintillators

With an aim to optimize ZnMoO_4 cryogenic scintillating bolometers, we have simulated the collection of scintillation photons in a detector module by a Monte Carlo method. A schematic view

Table 5
Radioactive contamination of ZnMoO_4 scintillators. Data on radioactive contamination of ZnMoO_4 [45,55] and ZnWO_4 [56] crystals are given for comparison.

Chain	Nuclide	Activity (mBq/kg)			
		ZnMoO_4		ZnWO_4	
		Present work	Ref. [45]	Ref. [55]	Ref. [56]
^{232}Th	^{232}Th	≤ 0.5	≤ 0.3	≤ 0.008	≤ 0.25
	^{228}Th	≤ 0.8	≤ 0.3	≤ 0.006	0.018(2)
^{235}U	^{227}Ac	≤ 0.5	–	–	0.011(3)
^{238}U	^{238}U	≤ 1.0	≤ 0.2	≤ 0.006	≤ 0.12
	^{234}U	≤ 0.8	≤ 0.8	≤ 0.011	–
	^{230}Th	≤ 0.8	≤ 0.3	≤ 0.006	≤ 0.16
	^{226}Ra	≤ 0.8	8.1(3)	0.027(6)	0.025(6)
	^{210}Po	8(1)	28(2)	0.70(3)	≤ 0.64
Total α activity		22 (2)	73(2)	–	2.3(2)

of the detector module is shown in Fig. 8. Using the GEANT4 package we have calculated light collection from ZnMoO_4 crystals of different shapes (cylindrical, hexagonal and octagonal), sizes (60 mm in diameter or in diagonal, by 20 and 40 mm height), surface treatment (polished and diffused), viewed by two photodetectors with diameters 20, 40 and 60 mm. A specular reflector with reflectivity 98% (3M) surrounds the ZnMoO_4 scintillator. We take into account the results of the index of refraction and emission spectrum measurements. We assume 30 cm of attenuation length in ZnMoO_4 crystals. The technique of the Monte Carlo simulation was tested with two ZnWO_4 crystal scintillators (of cylindrical and hexagonal shape) measured in different conditions of optical contact, reflector material, configuration and surface treatment [57].

As one can see from Table 6, crystal scintillators of hexagonal shape with diffused surface provide the best light collection. In addition, diffused scintillators also show much better uniformity of light collection. Octahedron scintillation elements show an intermediate level of light collection effectiveness. Using an octahedral shape could allow a compromise between the strong requirements of minimal wastes of rather expensive enriched material and a reasonable light collection to be reached.

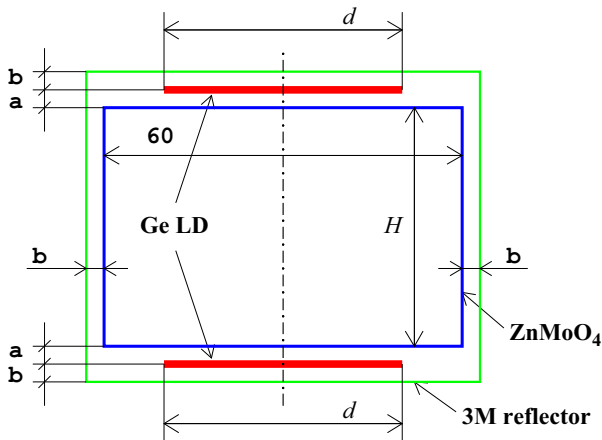


Fig. 8. Schematic view of optical module with ZnMoO_4 crystal scintillator 60 mm in diameter (diagonal of hexagonal, octahedron) with height H . “Ge LD” denotes Germanium light detectors with diameter d fixed at the distance a from the ZnMoO_4 crystal. Light reflector surrounds the module at the distance b from the ZnMoO_4 crystal surface and the light detectors, $a=b=3$ mm.

Table 6
Light collection from ZnMoO_4 crystal simulated with the help of the GEANT4 package.

Shape of ZnMoO_4 crystal	Size of crystal	Surface condition	Part of photons (%) reaching photodetectors with diameter (mm)		
			20	40	60
Cylinder	$\varnothing 60 \times 40$	Polished	2.6	6.7	11.8
		Diffused	3.6	11.0	20.5
	$\varnothing 60 \times 20$	Polished	4.3	10.6	16.8
		Diffused	7.7	21.9	36.5
Octahedron	60×40	Polished	3.5	8.4	14.3
		Diffused	3.9	11.9	22.6
	60×20	Polished	6.0	14.0	21.4
		Diffused	8.3	23.5	38.8
Hexagonal	60×40	Polished	3.8	9.1	15.3
		Diffused	4.2	12.7	24.0
	60×20	Polished	6.6	14.7	22.1
		Diffused	8.8	24.7	40.3

To describe the diffused surfaces we have used a diffuse reflection on a Lambertian surface. However, the real surfaces of inorganic crystals exhibit a combination of Lambertian and specular reflection. Therefore, the results of our calculations can be considered as estimations of an upper limit on the light collection.

5. Conclusions

Zinc molybdate (ZnMoO_4) single crystals were grown for the first time by the low-thermal-gradient Czochralski technique from additionally purified molybdenum. Measurements of optical transmission confirm a significant improvement of the optical properties of the crystal. There is no longer a broad absorption band with a maximum at ≈ 430 – 450 nm present in the transmission curves of the samples produced earlier [41,43]. The index of refraction of the material was determined for wavelengths in the range 406–655 nm. The crystal was found to be biaxial with refractive indexes in the range of 1.87–2.01.

Luminescence was measured under X-ray excitation in the temperature range 8–250 K with a maximum intensity at ≈ 110 – 140 K. When cooling to below 80 K, the light output drops by ≈ 3 – 4 times. The emission maximum of ZnMoO_4 occurs at 610 nm at room temperature and then shifts to 625 nm at 8 K. The sample studied shows intensive thermostimulated luminescence (TSL) at ≈ 75 K and intensive phosphorescence after irradiation of the sample at a temperature of 8 K. Both the phenomena indicate the presence of defects and impurities in the crystal. This shows that there are still margins of improvement of the quality of the material.

Scintillation and heat signals were simultaneously detected at low temperatures showing an excellent particle discrimination ability. With an acceptance of β events practically equal to 1, the α rejection factor is better than 10^{-3} at the energy of $0\nu 2\beta$ decay of ^{100}Mo .

Radioactive contamination of the ZnMoO_4 crystal was estimated by using data of cryogenic measurements. It confirms the improvement of ZnMoO_4 crystal radiopurity as a result of purification performed with the aim to enhance the optical quality of the material. Taking into account a much better radiopurity level of ZnWO_4 crystals (the total α activity of the best sample does not exceed the level of 0.2 mBq/kg [56]), one could conclude that radioactive contamination of ZnMoO_4 is mainly due to molybdenum. Therefore careful purification of molybdenum is necessary to produce radiopure ZnMoO_4 crystal scintillators.

Simulation of light collection from ZnMoO_4 crystal scintillators shows the advantages of hexagonal (or at least octahedral) crystal shape in comparison to cylindrical. Scintillators surfaces should be diffused to provide better light collection and uniformity.

Taking into account the substantial progress in ZnMoO_4 crystal production, we consider ZnMoO_4 crystals as promising low temperature phonon-scintillation detectors for large scale high sensitivity experiments to search for $0\nu 2\beta$ of ^{100}Mo , able to test the neutrino mass hierarchy.

R&D of large ZnMoO_4 crystals (up to 60 mm in diameter) and crystals from enriched ^{100}Mo is in progress.

Acknowledgments

The work of F.A. Danevich was supported by a Cariplo Foundation fellowship provided by the Landau Network – Centro Volta (Como, Italy). The groups from Orsay and Kyiv were supported in part by the project “Cryogenic detector to search for neutrinoless double beta decay of molybdenum” in the framework of the Programme “Dnipro” based on Ukraine-France Agreement on

Cultural, Scientific and Technological Cooperation. The analysis of the properties of Mo-based scintillating bolometers is part of the program of ISOTTA, a project receiving funds from the ASPERA 2nd Common Call dedicated to R&D activities. We also acknowledge Jack Mullins for his remarks regarding this manuscript.

References

- [1] F.T. Avignone III, S.R. Elliott, J. Engel, *Reviews of Modern Physics* 80 (2008) 481.
- [2] W. Rodejohann, *International Journal of Modern Physics E* 20 (2011) 1833.
- [3] S.R. Elliott, *Modern Physics Letters A* 27 (2012) 1230009.
- [4] J.D. Vergados, H. Ejiri, F. Simkovic, *Reports on Progress in Physics* 75 (2012) 106301.
- [5] A. Giuliani, A. Poves, *Advances in High Energy Physics* (2012) 857016.
- [6] A.S. Barabash, *Journal of Physics G* 39 (2012) 085103.
- [7] A. Alessandrello, et al., *Physics Letters B* 420 (1998) 109.
- [8] S. Pirro, et al., *Physics of Atomic Nuclei* 69 (2006) 2109.
- [9] P. Gorla, et al., *Journal of Low Temperature Physics* 151 (2008) 854.
- [10] L. Gironi, et al., *Optical Materials* 31 (2009) 1388.
- [11] I. Dafinei, et al., *IEEE Transactions on Nuclear Science NS-57* (2010) 1470.
- [12] C. Arnaboldi, et al., *Astroparticle Physics* 34 (2010) 143.
- [13] C. Arnaboldi, et al., *Astroparticle Physics* 34 (2011) 344.
- [14] S. Rahaman, et al., *Physics Letters B* 662 (2008) 111.
- [15] M.E. Wieser, J.R. De Laeter, *Physical Review C* 75 (2007) 055802.
- [16] V.A. Rodin, et al., *Nuclear Physics A* 766 (2006) 107.
- [17] V.A. Rodin, et al., *Nuclear Physics A* 793 (2007) 213.
- [18] M. Kortelainen, J. Suhonen, *Physical Review C* 76 (2007) 024315.
- [19] F. Simkovic, et al., *Physical Review C* 77 (2008) 045503.
- [20] A. Faessler, et al., *Journal of Physics G* 35 (2008) 075104.
- [21] J. Barea, F. Iachello, *Physical Review C* 79 (2009) 044301.
- [22] J. Kotila, et al., *Journal of Physics G* 37 (2010) 015101.
- [23] P.K. Rath, et al., *Physical Review C* 82 (2010) 064310.
- [24] T.R. Rodriguez, G. Martinez-Pinedo, *Physical Review Letters* 105 (2010) 252503.
- [25] R. Arnold, et al., *Physical Review Letters* 95 (2005) 182302.
- [26] L. Simard, on behalf of the NEMO-3 collaboration, *Journal of Physics: Conference Series* 375 (2012) 042011.
- [27] O.P. Barinova, et al., *Nuclear Instruments and Methods in Physics Research Section A* 613 (2010) 54.
- [28] L. Cardani, et al., arXiv:1307.0134 [physics.ins-det].
- [29] N.V. Bashmakova, et al., *Functional Materials* 16 (2009) 266.
- [30] H.J. Kim, et al., in: *Proceedings of New View in Particle Physics (VIETNAM'2004)*, August 5–11, 2004, p. 449.
- [31] S. Belogurov, et al., *IEEE Transactions on Nuclear Science NS-52* (2005) 1131.
- [32] A.N. Annenkov, et al., *Nuclear Instruments and Methods in Physics Research Section A* 584 (2008) 334.
- [33] S.J. Lee, et al., *Astroparticle Physics* 34 (2011) 732.
- [34] V.B. Mikhailik, et al., *Journal of Physics D* 39 (2006) 1181.
- [35] M. Minowa, et al., *Nuclear Instruments and Methods in Physics Research Section A* 320 (1992) 500.
- [36] Yu.G. Zdesenko, et al., *Pribory i Tekhnika Eksperimenta* 3 (1996) 53; Yu.G. Zdesenko, et al., *Instruments and Experimental Techniques*. 39 (1996) 364.
- [37] F.A. Danevich, et al., *Nuclear Instruments and Methods in Physics Research Section A* 622 (2010) 608.
- [38] L.I. Ivleva, et al., *Crystallography Reports* 53 (2008) 1087; L.I. Ivleva, et al., *Kristallografiya* 53 (2008) 1145.
- [39] W. Reichelt, et al., *Zeitschrift für Anorganische und Allgemeine Chemie* 626 (2000) 2020.
- [40] S.C. Abrahams, *Journal of Chemical Physics* 46 (1967) 2052.
- [41] L.L. Nagornaya, et al., *IEEE Transactions on Nuclear Science NS-56* (2009) 2513.
- [42] V.B. Mikhailik, et al., *Nuclear Instruments and Methods in Physics Research Section A* 562 (2006) 513.
- [43] D. Spassky, et al., *Physica Status Solidi A* 206 (2009) 1579.
- [44] L.G. Van Uiter, J.J. Rubin, W.A. Bonner, *Journal of the American Ceramic Society* 46 (1963) 512.
- [45] L. Gironi, et al., *Journal of Instrumentation* 5 (2010) P11007.
- [46] J.W. Beeman, et al., *Physics Letters B* 710 (2012) 318.
- [47] J.W. Beeman, et al., *Journal of Low Temperature Physics* 167 (2012) 1021.
- [48] J.W. Beeman, et al., *Astroparticle Physics* 35 (2012) 813.
- [49] A.A. Pavlyuk, et al., in: *Proceedings of the APSAM-92, Asia Pacific Society for Advanced Materials*, Shanghai, April 26–29, 1992, Institute of Materials Research, Tohoku University, Sendai, Japan, 1993, p. 164.
- [50] Yu.A. Borovlev, et al., *Journal of Crystal Growth* 229 (2001) 305.
- [51] E.N. Galashov, et al., *Crystallography Reports* 54 (2009) 689; E.N. Galashov, et al., *Kristallografiya* 54 (2009) 733.
- [52] D.A. Spassky, et al., *Optical Materials* 34 (2012) 1804.
- [53] J.W. Beeman, et al., *Nuclear Instruments and Methods in Physics Research Section A* 709 (2013) 22.
- [54] M. Tenconi, et al., *Bolometric light detectors for Neutrinoless Double Beta Decay search*, Presented at International Workshop on New Photon-Detectors (PhotoDet 2012), Laboratory of Linear Accelerator (LAL), Orsay, France, June 13–15, 2012, and in *Proceeding of Science PoS(PhotoDet-2012)072*.
- [55] J.W. Beeman, et al., *European Physical Journal C* 72 (2012) 2142.
- [56] P. Belli, et al., *Nuclear Instruments and Methods in Physics Research Section A* 626 (2011) 31.
- [57] F.A. Danevich, et al., *Optimization of light collection from crystal scintillators for cryogenic experiments*, *Nuclear Instruments and Methods in Physics Research Section A*, in preparation.